

DISCOVERY OF X-RAY EMISSION FROM G328.4+0.2, A CRAB-LIKE SUPERNOVA REMNANT

JOHN P. HUGHES¹

Department of Physics and Astronomy, Rutgers University, 136 Frelinghuysen Road, Piscataway NJ
08854-8019; jph@physics.rutgers.edu

PATRICK O. SLANE AND PAUL P. PLUCINSKY

Harvard-Smithsonian Center for Astrophysics, 60 Garden Street, Cambridge MA 02138

Received 2000 March 15; accepted 2000 May 8

ABSTRACT

G328.4+0.2 is a moderately small ($5' \times 5'$) Galactic radio supernova remnant (SNR) at a distance of at least 17 kpc that has been long suggested to be Crab-like. Here we report on the detection with *ASCA* of the X-ray emission from the SNR. The X-ray source is faint with an observed flux of $(6.0 \pm 0.8) \times 10^{-13}$ erg s⁻¹ cm⁻² over the 2–10 keV band. The emission is heavily cut-off at low energies and no flux is detected below 2 keV. Spectral analysis confirms that the column density to the source is indeed large, $N_{\text{H}} \sim 10^{23}$ atoms cm⁻², and consistent with the total column density of hydrogen through the Galaxy at this position. Good fits to the spectrum can be obtained for either thermal plasma or nonthermal power-law models, although the lack of detected line emission as well as other evidence argues against the former interpretation. The power-law index we find, $\alpha_P = 2.9_{-0.8}^{+0.9}$, is consistent with other Crab-like SNRs. In the radio band G328.4+0.2 is nearly as luminous as the Crab Nebula, yet in the X-ray band luminosity it is some 70 times fainter. Nevertheless its inferred soft X-ray band luminosity is greater than all but the brightest pulsar-powered synchrotron nebulae and implies that G328.4+0.2 contains a rapidly spinning, as yet undetected, pulsar that is losing energy at a rate of $\sim 10^{38}$ erg s⁻¹.

Subject headings: ISM: individual (G328.4+0.2, MSH 15–57) — pulsars: general — supernova remnants — X-rays: ISM

1. INTRODUCTION

Only about one-quarter of all cataloged Galactic radio-emitting supernova remnants (SNRs) (Green 1998) are known to emit X-rays based largely on observations by the *Einstein Observatory* and *ROSAT*. Some, and perhaps even many, of the non-detections are likely a result of the absorption of the typically soft (i.e., <2 keV) X-ray emission from SNRs by the large column density of gas and dust in the Galactic plane. However, young remnants, like Cassiopeia A, Tycho, and Kepler that show significant thermal emission above 2 keV, and pulsar-powered synchrotron nebulae, like the Crab Nebula with hard, featureless power-law spectra, should be able to shine through the interstellar medium. In fact the entire Galaxy is effectively transparent to X-rays with energies above about 4 keV. As part of an effort to identify and study such SNRs, we have targeted a sample of small diameter Galactic remnants with the *Advanced Satellite for Cosmology and Astrophysics* (*ASCA*), which has high sensitivity and moderate imaging capabilities in the hard X-ray band. Here we report on the discovery of X-ray emission from one of the remnants in the sample, G328.4+0.2.

G328.4+0.2 (MSH 15–57) has been cataloged as a radio SNR for quite some time (see, e.g., Clark & Caswell 1976) and, because of its flat radio spectrum, $S_{\nu} \propto \nu^{-0.24}$ (Milne 1979), and “filled-center” or plerionic morphology (Caswell et al. 1980; Whiteoak & Green 1996), it has long been considered as a possible Crab-like remnant. Its distance, based on H I absorption studies (Caswell et al. 1975; Gaensler, Dickel, & Green 2000 hereafter GDG), is rather large, 17 kpc or more, corrected to currently accepted val-

ues for the rotation curve and distance to the Galactic center. No pulsar has yet been detected (Kaspi et al. 1996) and previous searches for X-ray emission have been unsuccessful (Wilson 1986).

2. ANALYSIS

We observed G328.4+0.2 with *ASCA* (Tanaka, Inoue, & Holt 1994) on 17 March 1998. The solid-state imaging spectrometer (SIS), which comprises two separate arrays of CCD cameras, was operated in 2-CCD mode. The gas imaging spectrometer (GIS), consisting of two gas scintillation proportional counters, was operated in PH mode with the re-assignment of 2 bits of telemetry from pulse-height (compressing the spectra from 1024 channels to 256) to timing. This, in fact, resulted in no loss of spectral resolution since the GIS spectra are re-binned to this resolution before spectral analysis anyway. Rise-time information was used for suppressing background events. The data were screened using standard criteria that resulted in a combined exposure of 32900 s for the SIS detectors and 38950 s for the GIS detectors. The data from each detector were separately reduced and like observations were combined.

Images (see Figure 1) were made in two energy bands, which were chosen to optimize the signal-to-noise ratio of the detected sources. In each of the four sets of data (i.e., the two separate GIS and SIS detectors) two sources were apparent. One, a soft unresolved object, was detected with a statistical significance of 8.0σ in the SIS and 7.5σ in the GIS. This source is coincident with a previously known X-ray source from the *Einstein Observatory*,

¹ Also Service d’Astrophysique, L’Orme des Merisiers, CEA-Saclay, 91191 Gif-sur-Yvette Cedex France

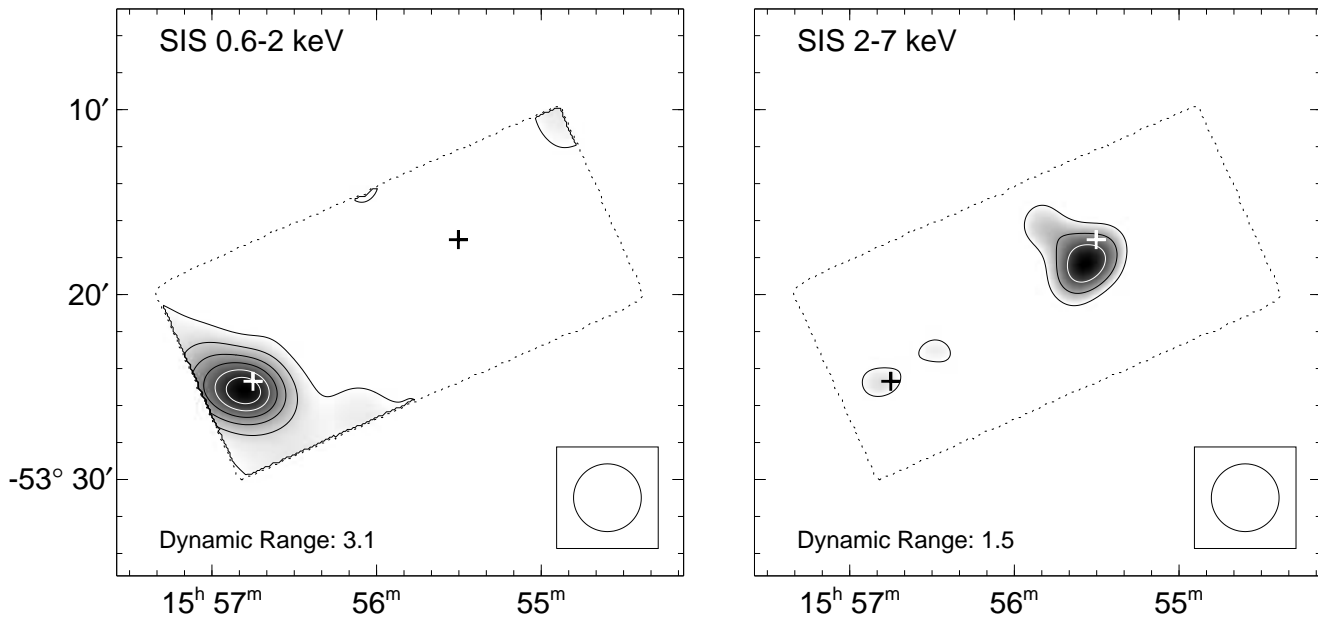


FIG. 1.— (a) X-ray image of the SNR G328.4+0.2 and environs from a 32900 s observation with the *ASCA* SIS in soft and hard X-ray bands as indicated. Plus signs denote the location of the radio SNR (the source to the west) and a previously known soft X-ray source. The data were smoothed with a $1'$ (σ) gaussian. In the soft band image, the greyscale runs linearly from 1.87×10^{-4} SIS counts s^{-1} arcmin $^{-2}$ (3σ above background) to 5.76×10^{-4} SIS counts s^{-1} arcmin $^{-2}$ (the peak emission). In the hard band image, the greyscale runs linearly from 3.00×10^{-4} SIS counts s^{-1} arcmin $^{-2}$ (3σ above background) to 4.55×10^{-4} SIS counts s^{-1} arcmin $^{-2}$ (the peak emission). In each panel contours are plotted at linear intervals from the minimum value to 90% of the peak. The dotted contour indicates the edge of the detector. The approximate size of the point-spread-function is indicated in the lower right.

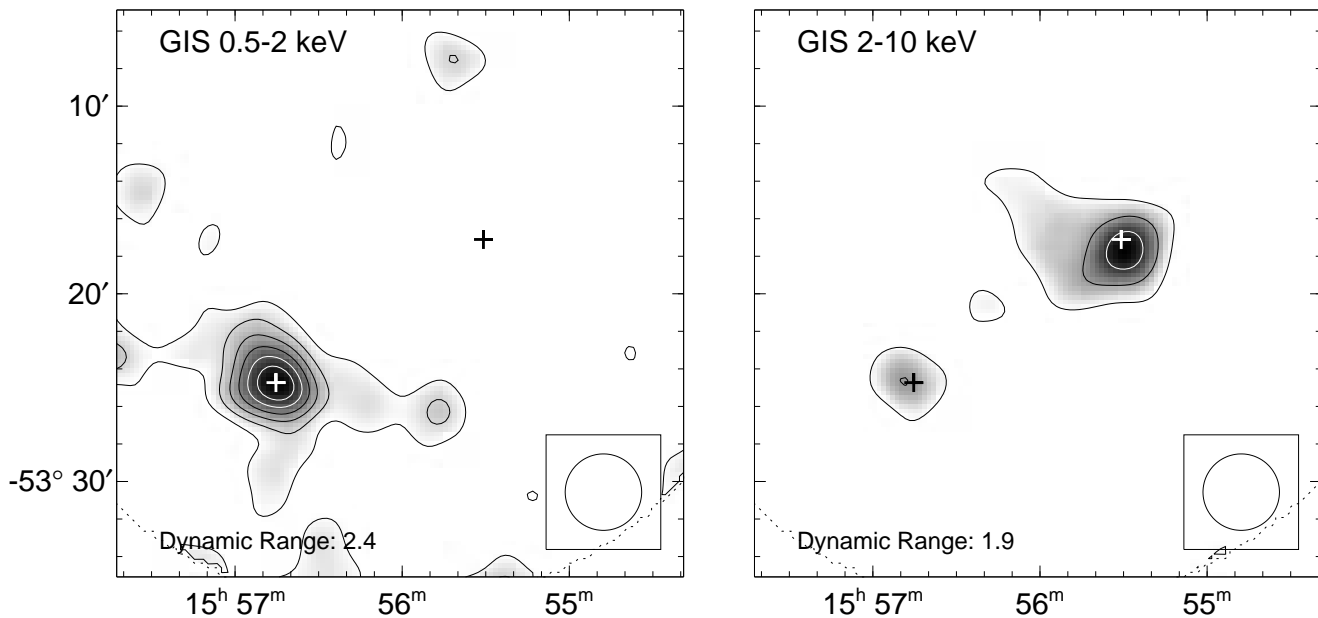


FIG. 1.— (b) Same as (a) except for the following. The data are from a 38950 s observation with the *ASCA* GIS. In the soft band image, the greyscale runs linearly from 1.19×10^{-4} GIS counts s^{-1} arcmin $^{-2}$ to 2.92×10^{-4} GIS counts s^{-1} arcmin $^{-2}$. In the hard band image, the greyscale runs linearly from 2.57×10^{-4} GIS counts s^{-1} arcmin $^{-2}$ to 5.01×10^{-4} SIS counts s^{-1} arcmin $^{-2}$.

2E 1552.8–5316, (Wilson 1986; Harris et al. 1990) and the *ROSAT* all sky survey, 1RXS J155644.7–532441 (Voges et al. 1999). We will not discuss this source any further, other than to note that it appears only in the band below 2 keV and is therefore likely to be a relatively nearby Galactic object.

In the band above 2 keV, at a position consistent with

that of G328.4+0.2, we detect a new X-ray source (designated AX J1555.5–5318) with a statistical significance of 8.4σ in the SIS and 8.5σ in the GIS. There are roughly 167 ± 20 SIS events and 222 ± 26 GIS events from the new source, which is unresolved at the spatial resolution afforded by the *ASCA* telescopes (i.e., roughly $3'$ half power diameter). There are no significant X-ray sources else-

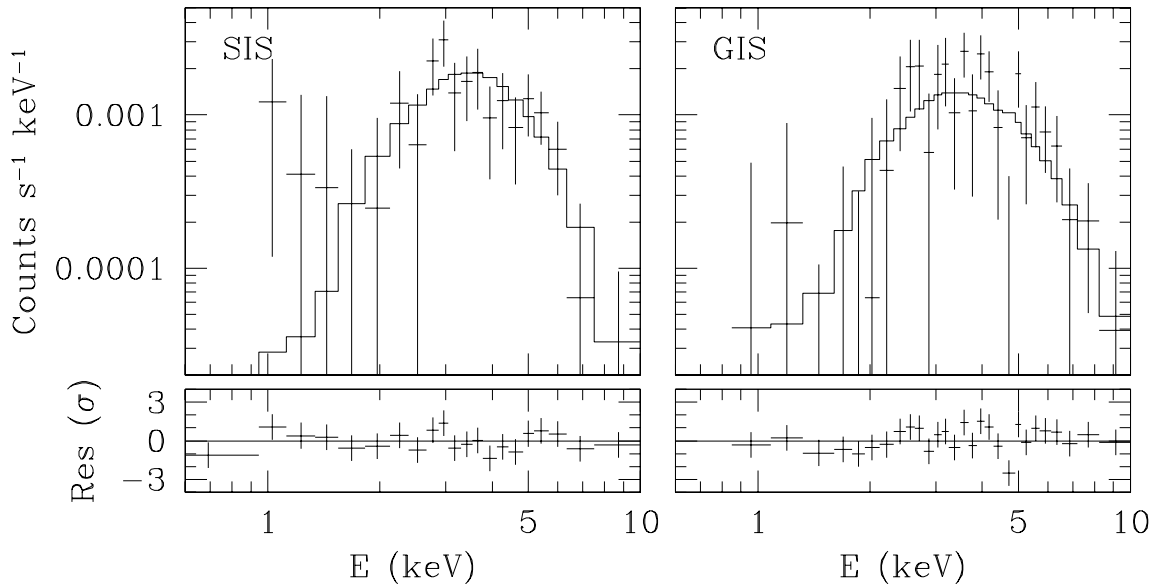


FIG. 2.— X-ray spectra of G328.4+0.2 from the *ASCA* SIS and GIS data as indicated. The best-fit power-law spectral model is shown as the histogram.

where in the fields of view of either the SIS or GIS other than the two we introduce above.

For completeness we carried out a search for coherent pulsations in AX J1555.5–5318 using the 2–10 keV GIS data. As a consequence of the re-assignment of some telemetry to timing information, as mentioned above, the time resolution of the GIS data was 0.015625 s and 0.125 s during the high and medium bit rate portions of the observation. These data were separately Fourier transformed (after correcting photon arrival times to the solar system barycenter) and the resulting power spectra were examined for significant peaks. The periods searched were 0.03125 s to 1024 s for the high time resolution data and 0.25 s to 4096 s for the medium time resolution data. No significant pulsed signal was detected, which is not surprising given the small number of source photons. We set a broad limit on the pulsed fraction of $\lesssim 50\%$.

Source and background spectra were extracted from both the SIS and GIS. The source regions were circles centered on the new X-ray source position with radii, chosen to optimize the signal-to-noise ratio of the extracted spectra, of 3/2 (SIS) and 3/9 (GIS). The background region for the SIS was taken from the apparently blank portion of the field of view surrounding the source toward the NW, SW, and SE (see Fig 1). For the GIS background we used an annular region centered on the position of the optical axis with inner and outer radii chosen so that the annulus just contained the circular source region. This was done to ensure that the background region contained emission that had experienced the same off-axis telescope properties (e.g., vignetting) as the source emission. Of course, both the source region and a region encompassing the X-ray emission from the other soft X-ray source were excluded from the GIS background annulus.

Local background regions were used because of concerns that diffuse emission from the well-known Galactic ridge emission (Worrall et al. 1982) might be present in the field

of view. In order to address this point the GIS spectra of the background regions were themselves studied using the new (point-source removed) blank-field background files from high Galactic latitudes. There is a clear excess of X-ray emission in the background regions near G328.4+0.2 that can be fit well by an absorbed thermal plasma model (Raymond & Smith 1977) with $kT \sim 6 - 7$ keV and a surface brightness of 1.3×10^{-4} counts s^{-1} arcmin $^{-2}$ or equivalently (in terms of flux over the 2–10 keV band) 1.1×10^{-14} ergs s^{-1} cm $^{-2}$ arcmin $^{-2}$. This is comparable to the brightness level expected for the ridge near this position. Our use of a local background is, therefore, not only justified but essential.

Response files for spectral fitting were generated employing standard software tools in the usual manner for *ASCA*. The combined SIS and GIS spectral data were re-grouped so that each spectral bin contained a minimum of 25 events in order to allow use of χ^2 as the figure-of-merit function for spectral fitting. Given the limited statistical quality of the data, only two simple spectral models were explored: an absorbed power-law and an absorbed thermal plasma model (Raymond & Smith 1977). The spectral data and power-law model are shown in Figure 2 and numerical values for the best-fit parameters are given in Table 1. A slightly better fit was obtained for the power-law model, although both models were statistically acceptable. The observed 2–10 keV band flux of the source is $(6.0 \pm 0.8) \times 10^{-13}$ erg s^{-1} cm $^{-2}$.

3. DISCUSSION

The large absorption we derive from both sets of spectral fits is fully consistent with the total Galactic column of hydrogen along the line-of-sight to G328.4+0.2, $N_{\text{H}} \sim 10^{23}$ atoms cm^{-2} . The column can be decomposed into three parts: (1) a neutral hydrogen column of $N_{\text{H}} \sim 3 \times 10^{22}$ atoms cm^{-2} (Wilson 1986), (2) an ionized hydrogen col-

TABLE 1
SPECTRAL MODEL FITS FOR G328.4+0.2

Parameter	Value and Error (1 σ)
Power-law Model	
N_{H} (H atoms cm^{-2})	$9.1^{+3.0}_{-2.4} \times 10^{22}$
α_{P}	$2.9^{+0.9}_{-0.8}$
$F_{\text{E}}(1 \text{ keV})$ (photon $\text{s}^{-1} \text{ cm}^{-2} \text{ keV}^{-1}$)	$1.8^{+6.0}_{-1.3} \times 10^{-3}$
$\chi^2/\text{d.o.f}$	37.6/48
Thermal Plasma Model	
N_{H} (H atoms cm^{-2})	$7.4^{+2.2}_{-1.7} \times 10^{22}$
kT (keV)	$4.0^{+4.5}_{-1.7}$
Fractional abundance (\odot)	<0.68 (90% C.L.)
Emission measure (cm^{-5})	$1.4^{+1.6}_{-0.6} \times 10^{11}$
$\chi^2/\text{d.o.f}$	38.2/47

umn of $N_{\text{HI}} \sim 3 \times 10^{22}$ atoms cm^{-2} estimated from the free-electron model of Taylor and Cordes (1993), and (3) a molecular hydrogen column of $N_{\text{H}_2} \sim 2 \times 10^{22}$ molecules cm^{-2} based on the CO data from Bronfman et al. 1989 and Bitran et al. 1997 (as reported by Slane et al. 1999). The agreement between these measures of the total hydrogen column supports the large distance of 17 kpc to this remnant derived from the H I absorption studies mentioned above.

3.1. Thermal Interpretation

The spectral fits themselves do not preclude a thermal interpretation for the X-ray emission from G328.4+0.2. However there are two main difficulties with the interpretation that cause us to disfavor it. First and foremost is the combination of a moderately high temperature and a lack of significant Fe-line emission. Mean plasma temperatures of greater than 2 keV tend to be the exception rather than the rule for SNRs and in all cases to our knowledge are accompanied by Fe K α line emission at ~ 6.7 keV. The second problem arises from the inferred evolutionary state of the remnant. It is possible to determine the age and explosion energy from the remnant's measured size, temperature, and emission measure in the context of similarity solutions for SNRs in the adiabatic phase of evolution (see, for example, Hughes, Hayashi, & Koyama 1998). The results are sensitive to assumptions about the state of equilibration between electrons and ions. If one assumes that the temperatures of the two species are fully equilibrated everywhere throughout the remnant, then the age and explosion energy of G328.4+0.2 are estimated to be 2000–4000 yr and $(0.9 - 1.8) \times 10^{51}$ erg, using values and uncertainty ranges from Table 1 and a total size of 2.5 in radius (GDG). Although these results are nicely consistent with expected values, various lines of evidence now suggest that full equilibration of electron and ion temperatures at supernova shock fronts is unlikely to be the correct scenario (Laming et al. 1996, Hughes et al. 1998). If one relaxes the assumption of full equilibration in favor of a scenario where Coulomb collisions regulate the exchange of energy between the species, then there are no plausible

solutions for the age and explosion energy of G328.4+0.2 (i.e., the inferred explosion energies are at least two orders of magnitude larger than the canonical value of 10^{51} erg). In summary, we consider it extremely unlikely that G328.4+0.2 is a young, thermally-emitting SNR.

3.2. Nonthermal Interpretation

Based on the radio properties of this SNR, specifically the filled-center morphology and high degree of linear polarization of the nebula ($\sim 20\%$; GDG), a nonthermal interpretation of the X-ray emission is most probable. And indeed the power-law index we find is consistent with that of other plerionic SNRs, of which the brightest and best known is the Crab Nebula with $\alpha_{\text{P}} = 2.1$ (Toor & Seward 1974). The nebular luminosity of such sources is powered by the spin-down energy loss of a rapidly-rotating young neutron star and the emission mechanism is synchrotron radiation from relativistic electrons in the presence of the magnetic field of the nebula. In some cases, like the Crab, pulsed radiation from the central compact star is observed, although in other cases it is not, perhaps due to unfavorable viewing geometry of the presumably beamed radiation from the pulsar. However, emission from the synchrotron nebula is isotropic and therefore, when detected, a synchrotron nebula is believed to provide clear evidence for the presence of a young pulsar.

The unabsorbed soft X-ray luminosity (0.2–4 keV band) of G328.4+0.2 is $\log(L_{\text{X}}/\text{erg s}^{-1}) = 35.6^{+1.0}_{-0.7}$. This value is larger than all known pulsar-powered synchrotron nebula with the exception of the Crab (Seward & Wang 1988), and two SNRs in the Large Magellanic Cloud: E0540–69.3 (Seward & Wang 1988) and N157B (Wang & Gotthelf 1998). It is comparable to the luminosities of the Crab-like cores of G29.7–0.3 (Blanton & Helfand 1996), G21.5–0.9 (Slane et al. 2000), and MSH 15–52 (Seward & Wang 1988). From the empirical relationship between the soft X-ray luminosity of the synchrotron nebula, L_{X} and the pulsar's rate of loss of rotational energy, \dot{E} (Seward & Wang 1988), we determine that the (still undiscovered) pulsar that must be powering the synchrotron emission is losing rotational energy at the rate of $\dot{E} \sim 10^{37} - 2 \times 10^{38} \text{ erg s}^{-1}$. GDG use

the radio luminosity to estimate a rotational energy loss rate of several $10^{38} \text{ erg s}^{-1}$. Given the large scatter in the correlations between \dot{E} and luminosity in each band, the differences between these estimates are unlikely to be significant. Indeed, focusing on the more interesting broad agreement between them, we conclude that G328.4+0.2 harbors a rapidly spinning pulsar that is losing rotational energy at a rate of $\sim 10^{38} \text{ erg s}^{-1}$.

GDG argue that the size and radio luminosity of G328.4+0.2 most closely resemble those of N157B, the SNR that contains the most rapidly spinning known pulsar with a period of 0.016 s (PSR 0537–6910; Marshall et al. 1998). This is also the case for the X-ray luminosity and for the ratio of X-ray to radio luminosity. The X-ray luminosity of the power-law component in N157B is $\log(L_X/\text{erg s}^{-1}) = 36.7$, at the upper end of our allowed range for G328.4+0.2. Although the ratio of X-ray to radio luminosity is low for G328.4+0.2, $L_X/L_R = 0.3 - 25$, nevertheless it is an excellent match to that of N157B ($L_X/L_R \sim 10$). In contrast L_X/L_R are 130 and 800 for the Crab and E0540–69.3, respectively. According to Wang & Gotthelf (1998) the X-ray synchrotron nebula in N157B is some 5×7 pc in size and is surrounded by a fainter diffuse component of thermal X-ray emission from the SN blast wave. Because of the broad point-spread-function of *ASCA*, we are unable to place interesting limits on the size of the X-ray synchrotron nebula in G328.4+0.2. This must await more sensitive and higher spatial resolution X-ray observations. Unfortunately, the large absorption toward G328.4+0.2 may forever preclude the detection of soft thermal X-ray emission (with $kT \sim 1$ keV) from any outer shell or blast wave in G328.4+0.2. We note that there is no evidence for a shell from the high spatial reso-

lution radio image (GDG).

The broadband spectrum of G328.4+0.2 from radio to X-ray frequencies is shown in Figure 3. The point at which the extrapolated best-fit radio and X-ray power-laws intersect, the so-called break frequency, is $\nu_B \sim 3 \times 10^{14}$ Hz. The large uncertainty on the measured X-ray spectral index results in a huge range for ν_B ($10^{11} \text{ Hz} - 6 \times 10^{15} \text{ Hz}$) that provides little more than consistency with values from other SNRs, e.g., the Crab with $\nu_B \sim 10^{13}$ Hz. Compared to the Crab, G328.4+0.2 is nearly as luminous in the radio band (GDG), while it is some 70 times less luminous in X-rays.

Synchrotron radiation theory (e.g., Ginzburg & Syrovatskii 1965) provides a means for estimating from the observed spectrum the amount of energy in relativistic particles and magnetic field in the nebula. One needs an additional constraint which we take to be the condition that the total energy is at a minimum. In this case the magnetic field energy is 3/4 of the energy in particles. We further assume that the energy in all relativistic particles is twice the energy in the electron component alone. We integrate the broadband spectrum (Fig. 3) from low frequency to ν_B using the radio spectral index and from ν_B to 2.4×10^{18} Hz (10 keV) using the X-ray spectral index. For our derived quantities we show explicitly the dependencies on distance, D , angular radius of the nebula, θ , the ratio of the energy in magnetic field to that in particles, κ_m , and the ratio of energy in all particles to electrons, κ_r . We use a value, $\theta = 1'$, for the size of the nebula that corresponds to the bright central portion (GDG). The value we derive for the nebular magnetic field is $B = 365 (\kappa_m/0.75)^{2/7} (\kappa_r/2)^{2/7} (D/17 \text{ kpc})^{-2/7} (\theta/1')^{-6/7} \mu\text{G}$ and the energy in relativistic electrons is $W_e = 5 \times$

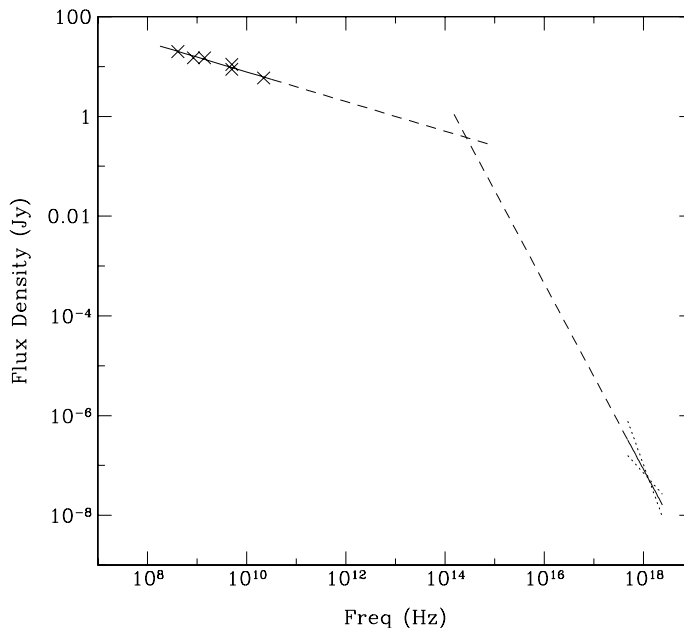


FIG. 3.— Broadband spectrum of G328.4+0.2 from radio to X-ray frequencies. Radio data points come from Caswell et al. (1975) (1.42 GHz); Clark & Caswell (1976) (0.408 GHz and 5 GHz). Tateyama, Sabalisk, & Abraham (1988) (5 GHz and 22 GHz); and Whiteoak & Green (1996) (0.843 GHz). The dashed curves show the extrapolation of the best-fit radio and X-ray power-law models to the point where they intersect at the so-called break frequency, which is $\sim 3 \times 10^{14}$ Hz (albeit with large errors).

$10^{49} (D/17 \text{ kpc})^2 (B/365 \mu\text{G})^{-3/2} \text{ erg}$, with roughly equal amounts of energy in the populations of electrons above and below the break frequency. Our estimates of the above quantities are reduced to $B \sim 220 \mu\text{G}$ and $W_e \sim 2 \times 10^{49} \text{ erg}$ if we use the lower limit on the break frequency (10^{11} Hz) that comes from the $1\text{-}\sigma$ lower limit on the X-ray spectral index. When the total energy in the nebula is computed, viz., $W = W_{cr} + W_B = \kappa_r(1 + \kappa_m)W_e$, even the lower limit value is still rather high, $W = 7 \times 10^{49} \text{ erg}$.

Although the energy we see currently in the synchrotron nebula must have come from the initial rotational energy of the pulsar, $E_0 = 2\pi^2 I P_0^{-2}$, it is also clear that W can represent only a fraction of E_0 . Some of the initial rotational energy of the pulsar has gone into radiation and the expansion of the nebula and some still remains in the form of the current spin of the pulsar. Calculating the precise partition of E_0 into the various forms that it may take is a challenging task and, given the limited quality of the current data, is beyond the scope of this work. Nevertheless by equating W to E_0 we can derive a strong upper limit to the initial spin period of the pulsar. Using $I = 10^{45} \text{ g cm}^2$ for the moment of inertia, the limit we obtain is $P_0 < 0.017 \text{ s}$. This limit is fully consistent with the current spin period of PSR 0537–6910 and adds further weight to the preceding arguments, as well as those in GDG, that the closest known analogue to G328.4+0.2 is the Crab-like SNR N157B.

4. CONCLUSIONS

Using *ASCA* we have discovered hard X-ray emission (2–10 keV band) from the Galactic radio SNR G328.4+0.2.

The new X-ray spectral data can be equally well fit by highly absorbed ($N_{\text{H}} \sim 10^{23} \text{ atoms cm}^{-2}$) thermal plasma or power-law models. When the inferred astrophysical properties of the remnant under each scenario are examined, along with additional constraints from recent radio observations, we conclude that G328.4+0.2 is a Crab-like SNR dominated by synchrotron emission in the radio and X-ray bands. It is powered by the spin-down energy of a central, yet undetected, pulsar that is currently losing energy at a rate of $\sim 10^{38} \text{ erg s}^{-1}$. In order to account for the total energy in particles and magnetic field observed in the synchrotron nebula at the present time, we find that the initial spin period of the pulsar must have been no more than 0.017 s. In many respects G328.4+0.2 bears a particularly close resemblance to the Crab-like SNR N157B in the Large Magellanic Cloud, the remnant containing the most rapidly rotating pulsar known, PSR 0537–6910. The discovery of its hidden pulsar is clearly an important next step in furthering our understanding of G328.4+0.2, yet the faintness of the remnant in the X-ray band ($6 \times 10^{-13} \text{ erg s}^{-1} \text{ cm}^{-2}$ over 2–10 keV) will make this search a challenging task.

This work made use of the SIMBAD Astronomical Database maintained by the Centre de Données Astronomiques de Strasbourg. Useful conversations with Cara Rakowski and Brian Gaensler are greatly acknowledged. We appreciate Monique Arnaud’s support and hospitality during the course of this project. Partial support was provided by NASA grant NAG5-6420 (JPH) and contract NAS8-39073 (POS, PPP).

REFERENCES

- Bitran, M., Alvarez, H., Bronfman, L., May, J., & Thaddeus, P. 1997, *A&AS*, 125, 99
 Blanton, E. L., & Helfand, D. J. 1996, *ApJ*, 470, 961
 Bronfman, L., Alvarez, H., Cohen, R. S., & Thaddeus, P. 1989, *ApJS*, 71, 481
 Caswell, J. L., Haynes, R. F., Milne, D. K., & Wellington, K. J. 1980, *MNRAS*, 195, 89
 Caswell, J. L., Murray, J. D., Roger, R. S., Cole, D. J., & Cooke, D. J. 1975, *A&A*, 45, 239
 Gaensler, B. M., Dicker, J. R., & Green, A. J. 2000, *ApJ*, submitted (GDG)
 Ginzburg, V. L., & Syrovatskii, S. I. 1965, *ARA&A*, 3, 297
 Green, D. A. 1998, ‘A Catalogue of Galactic Supernova Remnants (1998 September version)’, Mullard Radio Astronomy Observatory, Cambridge, U. K. (available on the World-Wide-Web at “<http://www.mrao.cam.ac.uk/surveys/snrs/>”)
 Harris, D. E., et al. 1990, The *Einstein Observatory* catalog of IPC X-ray sources, Smithsonian Astrophysical Observatory, Cambridge MA
 Hughes, J. P., Hayashi, I., & Koyama, K. 1998, *ApJ*, 505, 732
 Laming, J. M., Raymond, J. C., McLaughlin, B. M., & Blair, W. P. 1996, *ApJ*, 472, 267
 Kaspi, V. M., Manchester, R. N., Johnston, S., Lyne, A. G., & D’Amico, N. 1996, *AJ*, 111, 2028
 Marshall, F. E., Gotthelf, E. V., Zhang, W., Middleditch, J., & Wang, Q. D. 1998, *ApJ*, 499, L179
 Milne, D. K. 1979, *AuJPh*, 32, 83
 Raymond, J. C., & Smith, B. W. 1977, *ApJS*, 35, 419
 Seward, F. D., & Wang, Z. R. 1988, *ApJ*, 332, 199
 Slane, P. O., Chen, Y., Schultz, N., Seward, F. D., Hughes, J. P., & Gaensler, B. M. 2000, *ApJL*, 533, L29
 Slane, P. O., Gaensler, B. M., Dame, T. M., Hughes, J. P., Plucinsky, P. P., & Green, A. 1999, *ApJ*, 525, 357
 Tanaka, Y., Inoue, H., & Holt, S. S. 1994, *PASJ*, 46, L37
 Tateyama, C. E., Sabalick, N. S. P., & Abraham, Z. 1988, in *Supernova Remnants and the Interstellar Medium*, eds. R. S. Roger & T. L. Landecker (Cambridge: Cambridge University Press), p. 305
 Taylor, J. H., & Cordes, J. M. 1993, *ApJ*, 411, 674
 Toor, A., & Seward, F. D. 1974, *AJ*, 79, 995
 Voges, W., et al. 1999, *A&A*, 349, 389
 Wang, Q. D., & Gotthelf, E. V. 1998, *ApJ*, 494, 623
 Whiteoak, J. B. Z., & Green, A. J., *A&AS*, 118, 329
 Wilson, A. S. 1986, *ApJ*, 302, 718
 Worrall, D. M., Marshall, F. E., Boldt, E. A., & Swank, J. H. 1982, *ApJ*, 255, 111